



Biomechanical Modeling to Prevent Ischial Pressure Ulcers

Vincent Luboz, Marion Petrizelli, Marek Bucki, Bruno Diot, Nicolas Vuillerme, Yohan Payan

► To cite this version:

Vincent Luboz, Marion Petrizelli, Marek Bucki, Bruno Diot, Nicolas Vuillerme, et al.. Biomechanical Modeling to Prevent Ischial Pressure Ulcers. Journal of Biomechanics, 2014, pp.1-23. 10.1016/j.jbiomech.2014.05.004 . hal-00996034

HAL Id: hal-00996034

<https://hal.science/hal-00996034>

Submitted on 26 May 2014

HAL is a multi-disciplinary open access archive for the deposit and dissemination of scientific research documents, whether they are published or not. The documents may come from teaching and research institutions in France or abroad, or from public or private research centers.

L'archive ouverte pluridisciplinaire **HAL**, est destinée au dépôt et à la diffusion de documents scientifiques de niveau recherche, publiés ou non, émanant des établissements d'enseignement et de recherche français ou étrangers, des laboratoires publics ou privés.

Biomechanical Modeling to Prevent Ischial Pressure Ulcers

Vincent Luboz¹, Marion Petrizelli¹, Marek Bucki², Bruno Diot³, Nicolas Vuillerme⁴, Yohan Payan¹

¹ UJF-Grenoble1/CNRS/TIMC-IMAG UMR 5525, Grenoble, F-38041, France, {vluboz, ypayan}@imag.fr;

²TexiSense, Montceau-les-Mines, France, marek.bucki@texisense.com;

³IDS, Montceau-les-Mines, France, & Univ. Grenoble Alpes, Laboratoire AGIM FRE 3405 CNRS/UJF/UPMF/EPHE, La Tronche, France, b.diot@ids-assistance.com;

⁴ Univ. Grenoble Alpes, Laboratoire AGIM FRE 3405 CNRS/UJF/UPMF/EPHE, La Tronche, France & Institut Universitaire de France, Nicolas.Vuillerme@agim.eu

Corresponding author:

Yohan Payan
Equipe GMCAO - Laboratoire TIMC-IMAG
Université Joseph Fourier - CNRS UMR 5525
Pavillon Taillefer
Faculté de Médecine - 38706 La Tronche cedex - France
Tel: +33 (0)4 56 52 00 01 - Fax: +33 (0)4 56 52 00 55
email: yohan.payan@imag.fr

Keywords: pressure ulcer prevention, biomechanical model, stiffness influence, spinal cord injury.

To appear in *Journal of Biomechanics* (2014)

27 **Abstract**

28 With 300,000 paraplegic persons only in France, ischial pressure ulcers represent a major
29 public health issue. They result from the buttocks' soft tissues compression by the bony
30 prominences. Unfortunately, the current clinical techniques, with – in the best case –
31 embedded pressure sensor mats, are insufficient to prevent them because most are due to high
32 internal strains which can occur even with low pressures at the skin surface. Therefore,
33 improving prevention requires using a biomechanical model to estimate internal strains from
34 skin surface pressures. However, the buttocks' soft tissues' stiffness is still unknown. This
35 paper provides a stiffness sensitivity analysis using a finite element model. Different layers
36 with distinct Neo Hookean materials simulate the skin, fat and muscles. With Young moduli
37 in the range [100 - 500 kPa], [25 - 35 kPa], and [80 - 140 kPa] for the skin, fat, and muscles
38 respectively, maximum internal strains reach realistic 50 to 60 % values. The fat and muscle
39 stiffnesses have an important influence on the strain variations, while skin stiffness is less
40 influent. Simulating different sitting postures and changing the muscle thickness also result in
41 a variation in the internal strains.

42

44 **1. Introduction**

45 With more than 300,000 paraplegic persons only in France among which 80 % will
46 develop a pressure ulcer in their life because they do not change posture by reflex, preventing
47 ischial pressure ulcer is critical. Pressure ulcers start at the interface between bones and soft
48 tissues underneath an intact skin and advance outwards rapidly causing substantial
49 subcutaneous damages before being visible at the skin surface. Usual prevention in the
50 clinical routine consists in using cushions to reduce the pressure below the patients' buttocks
51 and regularly changing their sitting posture. This procedure is not always effective as it
52 demands a constant monitoring. When prevention fails, pressure ulcers develop and patients
53 must stay in bed for months before healing and/or undergo heavy surgery.

54 Measuring surface pressures can help in alerting users against skin injuries (Pipkin and
55 Sprigle, 2008), but these measurements cannot predict dangerous internal tissue loadings
56 (Linder-Ganz et al., 2008) responsible for most of the deep pressure ulcers. For example, a
57 similar pressure map may be observed under the buttocks of a heavy paraplegic person with
58 sharp ischial tuberosity (IT) and a thin person with blunt ITs; however, deep pressure ulcer
59 formation depends on the IT curvature as well as the thickness of the soft tissues (Sopher et
60 al., 2010). Quantitatively estimating the internal strains from the interface pressures while
61 taking into account the anatomical variability is only possible by (1) building a patient-
62 specific biomechanical model of the soft tissues/bony prominence and (2) using this
63 numerical model to compute the internal strains (Elsner and Gefen, 2008, Loerakker et al.,
64 2011).

65 Several biomechanical models of the gluteal region have already been proposed. (Linder-
66 Ganz et al., 2009) proposed a 2D biomechanical model using a Neo Hookean constitutive law

67 for the muscles ($E = 31$ kPa, $\nu = 0.49$) and the other soft tissues ($E = 9$ kPa, $\nu = 0.49$) to
68 evaluate the internal strains in the buttocks of a paraplegic patient. This study was completed
69 by a MRI analysis (Shabshin et al., 2010) of several patients and showed an average maximal
70 internal strain of 72 % for the muscles and 35 % for the fat tissues when the subjects sit on a
71 rigid chair. While sitting on a softer material (foam), the average maximal internal strain
72 decreases to 64 % for the muscles and to 23 % for the fat tissues. (Oomens et al., 2003)
73 presented a 2D biomechanical model of the buttock with a simplified ischium and three layers
74 of tissues (skin, fat and muscles) modeled with an Ogden material ($\alpha_{\text{skin}} = 10$, $\mu_{\text{skin}} = 8$ kPa,
75 $\alpha_{\text{fat}} = 5$, $\mu_{\text{fat}} = 10$ kPa, $\alpha_{\text{muscle}} = 30$, $\mu_{\text{muscle}} = 3$ kPa). The simulation showed that the maximal
76 internal strain, when lying on a cushion, was below the IT in the fat layer. Another study from
77 (Verver et al., 2004) used a Neo Hookean constitutive law to model the skin ($E = 150$ kPa, $\nu =$
78 0.46) and a Mooney Rivlin constitutive law to model the other soft tissues ($A_1 = 1.65$ kPa,
79 $A_2 = 3.35$ kPa, $\nu = 0.49$) in a 3D biomechanical model. It showed that the pressure
80 distribution depends on the stiffness of the chair cushion, on the stiffness of the buttocks' soft
81 tissues, and on the posture of the subject. A three-value sensitivity analysis of the stiffness
82 was performed for the soft tissue layer (muscle and fat combined), showing some influences
83 on the resulting stresses.

84 It appears that the literature has proposed many values for stiffness parameters as well as
85 various modeling hypotheses (homogeneous model, different layers with or without the
86 skin...) from one study to the other. In order to quantify these differences, this paper presents
87 a sensitivity analysis of the buttocks soft tissues' stiffness using a 3D biomechanical model of
88 the gluteal soft tissues in sitting position. The study separates the soft tissues in different
89 materials for each of the three layers of the buttocks: skin, fat, and muscles. The mechanical
90 parameter ranges are defined iteratively. The algorithm starts with the values found in the
91 literature and refines them in order to obtain an average deformation between 50% and 60 %,

considering the range of maximal internal VM strains observed in the literature (Linder-Ganz et al., 2009, Oomens et al., 2003, Shabshin et al., 2010, Verver et al., 2004), within a patient-specific model. The second part of the study focuses on two different sitting postures and on the influence of the muscle layer thickness.

2. Materials and Methods

The first step of this study is to build the finite element (FE) mesh from a dataset. The boundary conditions are defined before specifying the different material properties applied to the buttocks soft tissues. The modeling and simulation are performed within the ArtiSynth open source framework (Lloyd et al., 2012) (www.artisynth.org).

a. Creation of the finite element mesh

The anatomy of our model is extracted from the dataset of a young healthy male subject (38 years old, 100 Kg and 1.90 m). The subject's CT exam (image size 512x512x403, and resolution 0.97x0.97x1 mm³, fig. 1d) was semi-automatically segmented to acquire the external surfaces of the skin, the muscles and the bones, using the ITK-Snap software's snake segmentation (Yushkevich et al., 2006). Because the subject was lying on his right side (which was therefore compressed), only his left buttock was segmented. The right side was reconstructed by symmetry. The muscles were segmented as a single entity as it was too difficult to separate them on the dataset.

Using an automatic hexahedrons-dominant FE mesh generator (Lobos et al., 2010), the segmented skin surface was filled with finite elements as illustrated in fig 1a. Because we assume the bones to be rigid, they are represented as non-deformable solids. The different layers are also taken into account by this mesh generator which creates a finite element mesh

with clear and precise boundaries between each of them, fig. 1b and c. The mesh is composed of 164,690 linear elements (including 45,374 hexahedrons, 40,470 pyramids, 54,778 tetrahedrons, and 24,068 wedges) and 89,136 nodes.

b. Boundary conditions

In our simulation, gravity is not taken into account since it was shown that its influence is limited when buttocks are in a sitting configuration (there is at least a 100 fold difference between the influence of the subject weight on the whole buttocks and the influence of the gravity when applied to those tissues). The finite element nodes at tissue/bone interface are fixed, fig. 1b and c, as a no sliding binding between the soft tissues and the bones is assumed.

The model is subject to a set of pressures measured with a commercial pressure sensor (www.zebris.de, with 50x51 sensors of 0.8 cm² each). The subject was sitting on the sensor with the feet not touching the ground and his back not on the chair rest so that all his weight was on the pressure sensor, his arms crossed on his chest. The recorded pressure map is shown on fig 2. The highest pressure reaches 4 N.cm⁻². The finite element nodes of the skin surface are orthogonally projected onto this pressure map to determine the pressure values for each of them. To ensure the convergence of the simulation this pressure is applied as a linear ramp from 0 % of the pressure at 0.1 s to 100 % of the pressure at 1.1 s. The pressure is applied along the normal at each of the nodes and taking into account the surface of the neighboring elements. These normal and surface are recomputed at each time step.

c. Buttocks model

In order to enhance the anatomical realism of the model, the three main soft structures of the buttocks are considered for the finite element model, namely the skin, fat, and muscles. Fig 1b and c show cross sections of the mesh after identifying these structures. There are

83,001 elements in the fat layer, 73,623 in the muscle layer and 8066 in the skin layer. The first step consists of representing the skin as a thin layer of elements at the outer surface of the finite element mesh built in section 2.a. This 1.5 mm layer (Hendriks et al., 2006) is extruded from the finite element mesh. It results in a 1-element thick layer representing the skin.

In a second step, the elements representing the muscle layer, fig 1b and c, are identified by finding the elements of the finite element mesh located inside the muscle surface segmented from the medical dataset. Finally, the elements between the skin layer and the muscle layer are considered as fat tissues.

These three layers are modeled using a compressible Neo Hookean constitutive material (Bonnet & Wood, 1997). Such material exhibits characteristics that can be identified with the familiar material parameters found in linear elastic analysis. Its energy function depends on the two Lamé parameters and can also be expressed as a function of the shear and bulk modulus as well as a function of the Young modulus E and Poisson's ratio ν (see Bonnet & Wood, 1997 for details). We have chosen in this paper to provide E and ν values so that the material can be compared with other constitutive materials proposed in the literature. Since the main objective of our study was to provide a sensitivity analysis as concerns the tissues' stiffness (modeled with the Young modulus), a fixed value of 0.49 was assumed for the Poisson's ratio. This value was already proposed by other groups (Linder-Ganz et al., 2009, Verver et al., 2004) since it has the advantage of representing the quasi-incompressibility for the buttocks soft tissues. To evaluate the influence of the stiffness parameters of each layer, a sensitivity analysis was carried out by setting the layers' Young moduli to different values ranging from 5 to 40 kPa for the fat layer (every 5 kPa), from 40 to 160 kPa for the muscles (every 20 kPa), and from 100 to 500 kPa for the skin (every 100 kPa). Those values were chosen according to the ones reported in the literature.

d. Evaluation of three different sitting postures

Based on the existing literature (Linder-Ganz et al., 2009, Oomens et al., 2003, Shabshin et al., 2010, Verver et al., 2004), further simulations are carried out, using the “reference” constitutive parameters derived from the biomechanical model. From this model, a study of the influence of two different sitting postures is performed: in the initial position (with the trunk forming a 110 degree angle with the legs) and in a more upright sitting position (with the body forming a 90 degree angle with the legs). To perform this change of angle, the segmented surface of the skin and bones are deformed using the lattice tool in Blender (blender.org). The same pressure map is applied in both cases.

A second posture test is performed by comparing the initial sitting posture constrained with the initial pressure map, fig 2, and the initial sitting posture constrained with a different pressure map of the same healthy young subject. In this case, the subject’s weight is deported to his right side, fig 3, to simulate unilateral sitting posture. Comparing those two postures allows simulating the change of postures that a paraplegic patient might experience during the day.

Finally, the influence of the thickness of the muscle layer is also considered in the initial sitting posture (with the 110 degree angle). The muscle layer is reduced by 10 mm and 20 mm (from about 19 cm at its most) to study the consequences of the decrease of its thickness in conjunction with the increase of fat thickness. These simulations were chosen because the subject who participated to the development of our biomechanical model is young and healthy and consequently has a fairly important layer of muscles whereas older and/or paraplegic patients may have thinner muscle layers.

3. Results

As mentioned in the introduction, pressure ulcers are due to high internal strains even though low pressures are measured at the skin surface. The risk of formation of a pressure ulcer should therefore be assessed based on the level of maximal internal strains in the FE mesh. The strain measure commonly used in the literature is the Von Mises (VM) equivalent strain (Linder-Ganz et al., 2008, Oomens et al., 2003). Based on the work of (Loerakker et al., 2011), another criterion, namely the volume of the largest zone with contiguous nodes with VM strains over 20 %, was measured during the simulations and is discussed in the appendix.

a. Buttocks model sensitivity analysis

The influence of the Young moduli chosen for the three types of soft tissues is displayed in figure 4 which shows the maximal VM strains below the ischial tuberosities for the 245 simulations made with different Young moduli defined for the skin (E_{skin}), fat (E_{fat}), and muscle (E_{muscle}) layers. From left to right, the fat Young's modulus varies from 10 kPa to 40 kPa. For a given fat Young's modulus, the moduli for the skin and muscle vary respectively from 100 kPa to 500 kPa and from 40 to 160 kPa.

An example of a map of the maximal VM strains is given in Figure 5. It shows that they are located below the IT, in the fat layer, close to the muscle/fat interface. This is the case for most of the simulations. It must be noted that occasionally the maximal VM strains are located inside the muscle layer, close to the bone/muscle interface, when the muscles' Young's modulus is close to the fat's Young's modulus, for example when $(E_{\text{muscle}}, E_{\text{fat}}) = (40 \text{ kPa}, 40 \text{ kPa})$ or $(E_{\text{muscle}}, E_{\text{fat}}) = (60 \text{ kPa}, 40 \text{ kPa})$.

As concerns the Young moduli chosen for the fat, it appears that values below 20 kPa lead to huge strains (more than 100%), far above the deformations mentioned in the literature. It seems therefore that such values are not realistic.

Looking at figure 4 in more details, it appears that the strains levels are not very sensitive to the Young moduli chosen for the skin tissues. Indeed, with skin moduli ranging between 100 and 500 kPa, there is an average variation of 3.7 % of the VM strains with a standard deviation of 3.3 percentage points (PPs). The minimum VM strains variation is 0.1% for $(E_{\text{muscle}}, E_{\text{fat}}) = (120 \text{ kPa}, 40 \text{ kPa})$ while the maximum VM strains variation only reaches 17.1 % for $(E_{\text{muscle}}, E_{\text{fat}}) = (40 \text{ kPa}, 10 \text{ kPa})$.

On the contrary, the strain sensitivity to the Young's modulus of the muscle is more important with a VM strain variation of 38.5 % with a standard deviation of 15.9 PPs. For E_{muscle} 's range, minimum and maximum VM strains of 1.5 % and 54.8 % are measured respectively for $(E_{\text{fat}}, E_{\text{skin}}) = (5 \text{ kPa}, 500 \text{ kPa})$ and $(40 \text{ kPa}, 500 \text{ kPa})$. Finally, the most sensitive parameter is the Young's modulus of the fat with a strain variation of 71.1 % and a standard deviation of 21.6 PPs. For E_{fat} 's range, minimum and maximum VM strains of 22.8 % and 92.7 % are measured for respectively $(E_{\text{muscle}}, E_{\text{skin}}) = (40 \text{ kPa}, 100 \text{ kPa})$ and $(160 \text{ kPa}, 100 \text{ kPa})$. Overall, it appears that the influence of the skin stiffness can be neglected compared to ones of the fat and muscle, among which the influence of fat stiffness is the most important.

Finally, considering the range of maximal internal VM strains observed in the literature and in Figure 4 (i.e. between 50 % and 60 %), the following material parameter values could lead to these deformations and are therefore assumed to be realistic: E_{skin} in the range [100 - 500 kPa], E_{fat} in the range [25 - 35 kPa], and E_{muscle} in the range [80 - 140 kPa].

In the rest of the paper, we propose to define a “reference” set of values inside these realistic ranges, namely $E_{\text{skin}} = 200 \text{ kPa}$, $E_{\text{fat}} = 30 \text{ kPa}$, and $E_{\text{muscle}} = 100 \text{ kPa}$. These values lead to a maximal strain of 57.4 %. They will be used as a reference for the simulations provided to study the influence of two different sitting postures and muscle layer thickness.

b. Consequences of the different sitting postures on the internal VM strains

The two sitting postures described in section 2.d (on one side or sitting upright) are simulated in order to evaluate their respective effect on the maximal internal strains. As mentioned above, those simulations are performed with the biomechanical model using the “reference” parameters.

When sitting in the upright position, the maximal internal strain observed is 64.1 %, which represents an increase of 6.7 VM strain PPs compared to the initial position (a maximal VM strain of 57.4 % was observed at 110 degrees).

When sitting on the right side of the buttocks - a situation represented by the pressure map of fig. 3 - the maximal internal strain observed is 64.2 %, which represents an increase of 6.8 VM strain PPs compared to the initial position (where the buttocks are evenly positioned on the platform with an angle of 110 degrees).

c. Effect of the variation of muscle thickness on internal strains

To assess the influence of the thickness of the muscle layer on maximal VM strains, two new biomechanical models were created by reducing the muscle thickness by 10 mm and 20 mm, as explained in section 2.d. Note that by consequences, the fat layer thickness increases by 10 and 20 mm. Again, the simulations are performed with the “reference” mechanical parameters.

With 10 mm and 20 mm muscle layer thinnings, maximal internal VM strains of 71.9 % and 97.7 % are observed respectively, which represent an increase of 14.5 and 40.3 PPs compared to the initial case. Those maximal strains are again located below the IT, in the fat layer, close to the muscle/fat interface. Of course, because of the reduction of the muscle thickness, this interface is closer to the bony structure than in the initial model.

4. Discussion and conclusion

A subject-specific 3D finite element biomechanical model of the buttocks was introduced to study the influence of material stiffness, soft tissue layers thicknesses and postures onto internal strains. The model is built from the segmentation of a CT scan which provided the surfaces of the skin, muscles and bones. It includes the main structures that constitute the buttock soft tissues, namely the skin, fat and muscles. This model uses a compressible Neo Hookean constitutive law, with a Poisson ratio of 0.49. A wide range of Young moduli was implemented to evaluate the influence of each soft tissue layer ($E_{\text{fat}} = 10$ to 40 kPa, $E_{\text{muscles}} = 40$ to 160 kPa, and $E_{\text{skin}} = 100$ to 500 kPa). These evaluations show that the skin layer has little influence on the maximal strains. This is probably due to the fact that this layer is very thin and quite stiff. On the other hand, because of their comparatively large thicknesses and lower stiffnesses, the fat and muscle layers have much more influence. Based on the results for this subject and given the maximal VM strains observed in the literature, a maximal internal strain between 50 and 60 % was assumed to be the most realistic one and was obtained with E_{skin} in the range [100 - 500 kPa], E_{fat} in the range [25 - 35 kPa], and E_{muscle} in the range [80 - 140 kPa]. Furthermore, this sensitivity analysis shows that the maximal VM strains are mainly located below the IT, in the fat layer, close to the muscle/fat interface. This tissue will consequently be suffering the most from pressure ulcers. The maximal VM strains occasionally appear inside the muscle layer, close to the bone/muscle interface, but only when the muscles' Young's modulus is similar to the fat's Young's modulus, which is probably the case for paraplegic or elderly persons.

This study also allowed evaluating the influence of three different sitting postures: sitting with a 110 degree angle between legs and torso (initial posture), sitting with a 90 degree angle between legs and torso (upright), and sitting only on the right side of the buttocks. Simulations showed that sitting in the upright posture increases the maximal internal

VM strain by 6.7 PPs as compared to 57.4 %. This could be explained by the position of the ischial tuberosity: at 90 degrees, the ischia protrude more and probably act more like picks stabbing the soft tissues than in the 110 degree sitting posture. The displacements of the cushioning muscle layer with respect to the more or less protruding ischia, not simulated here, should also be considered as a possible cause. This observation could be different for other subjects because of the distinct morphology of their ischia or different soft tissues layer thicknesses. When sitting on the right side of the buttocks, the maximal internal strain increases by 6.8 PPs compared to the initial posture. This increase is due to the weight transfer on the right side. Intuitively, a larger increase could be expected. This discrepancy can be explained by the fact that the subject's total weight was not only transferred on his right buttocks, but also on his right leg (light blue zone on fig. 3), which is not included in our model. Therefore the recorded pressure pattern does not reflect an unsupported unilateral weight transfer and the resulting strains are probably lower than they should be. This observation indicates that the buttocks model should consequently be extended to include the upper thigh.

Finally, the influence of the muscle layer thickness has been studied by reducing it by 10 and 20 mm. It showed an increase of the maximal internal strains by 14.5 and 40.3 VM strain PPs, respectively. The location of those strains in the fat layer below the ischia indicates that paraplegic patients with a thinner muscle layer or fatter patients might be more likely to develop a pressure ulcer. Again, this has to be verified on more than one subject but this conclusion is in accordance with Gefen and colleagues' studies (Elsner and Gefen, 2008, Sopher et al., 2010).

Overall, using our biomechanical model allows studying the formation of pressure ulcers and could help developing different strategies to prevent them. To this aim, the use of a pressure sensor mat embedded on the patient wheelchair and coupled with a biomechanical

model seems relevant provided that such a model is able to evaluate in real time the gluteal tissues internal strains and consequently to raise warnings in case of pressure ulcers risks.

Nevertheless, before proposing such pressure ulcer prevention tools for a routine use, several points still need to be improved. The first one is the necessity, for each patient modeled with our method, to automatically import patient-specific data: anatomical surfaces and biomechanical parameters. It is indeed critical to be able to differentiate each tissue layer, especially the skin, muscles, and the bones, as their positions can play a key role in the location of pressure ulcers. Other imaging modalities with corresponding image processing would probably have to be studied to improve this point. Finally, the definition of the patient-specific mechanical parameters will also need to be addressed since soft tissue stiffness, especially for the fat and muscle tissues, impacts significantly the range of internal strains and consequently the risks for pressure ulcer formation. Using elastography (from MRI or Ultrasound) or classical indentation could help in estimating these elastic parameters in vivo. It could also help in defining a more precise Poisson ratio as the value chosen in this study is for now inspired by the literature. A preliminary sensitivity analysis of this parameter indeed showed large variations of the VM strains even with small variations of the Poisson ratio (as pointed in Gefen, 2010).

5. Acknowledgments

This work is partly funded by the French national project ANR, under reference ANR-TecSan 2010-013 IDS, by the Institut Universitaire de France, and by French state funds managed by the ANR within the Investissements d'Avenir programme (Labex CAMI), under reference ANR-11-LABX-0004.

Conflict of interest statement: the authors certify that no conflict of interest is raised by this work.

6. References

Bonet, J., and Wood, R.D., 2008. Nonlinear Continuum Mechanics for Finite Element Analysis. Cambridge University Press.

Elsner, J.J., and Gefen, A., 2008. Is obesity a risk factor for deep tissue injury in patients with spinal cord injury? *Journal of Biomechanics*, 41:3322–3331.

Gefen A., 2010. The biomechanics of heel ulcers. *J Tissue Viability*, 19(4):124-31.

Hendriks, F.M., Brokken, D., Oomens, C.W.J., Bader, D.L., and Baaijens, F.P.T., 2006. The relative contributions of different skin layers to the mechanical behavior of human skin in vivo using suction experiments. *Medical Engineering & Physics*, 28:259–266.

Linder-Ganz, E., Shabshin, N., Itzhak, Y., Yizhar, Z., Siev-Ner, I., and Gefen, A., 2008. Strains and stresses in sub-dermal tissues of the buttocks are greater in paraplegics than in healthy during sitting. *Journal of Biomechanics*, 41:567–580.

Linder-Ganz, E., Yarnitzky, G., Yizhar, Z., Siev-Ner, I., and Gefen, A., 2009. Real-Time Finite Element Monitoring of Sub-Dermal Tissue Stresses in Individuals with Spinal Cord Injury: Toward Prevention of Pressure Ulcers, *Annals of Biomedical Engineering*, 37(2):387–400.

Lloyd, J.E., Stavness, I., and Fels, S., 2012. Artisynth: a fast interactive biomechanical modeling toolkit combining multibody and finite element simulation. In: Payan Y. (Ed.), *Soft Tissue Biomechanical Modeling for Computer Assisted Surgery*, Studies in Mechanobiology, Tissue Engineering and Biomaterials, 11:355–394.

353 Lobos, C., Payan, Y., and Hitschfeld, N., 2010. Techniques for the generation of 3D Finite
 354 Element Meshes of human organs. *Informatics in Oral Medicine: Advanced Techniques in*
 355 *Clinical and Diagnostic Technologies*. Hershey, PA: Medical Information Science Reference,
 356 126-158.

357 Loerakker, S., Manders, E., Strijkers, G.J., Nicolay, K., Baaijens, F.P.T., Bader, D.L.,
 358 Oomens, C.W.J., 2011. The effects of deformation, ischaemia and reperfusion on the
 359 development of muscle damage during prolonged loading. *Journal of Applied Physiology*,
 360 111(4): 1168-1177.

361 Oomens, C.W.J., Bressers, O.F.J.T., Bosboom, E.M.H., Bouten, C.V.C. and Bader, D.L.,
 362 2003. Can Loaded Interface Characteristics Influence Strain Distributions in Muscle Adjacent
 363 to Bony Prominences? *Computer Methods in Biomechanics and Biomedical Engineering*,
 364 6(3):171-180.

365 Pipkin, L., and Sprigle, S., 2008. Effect of model design, cushion construction, and interface
 366 pressure mats on interface pressure and immersion. *Journal of Rehabilitation Research &*
 367 *Development*, 45:875–882.

368 Shabshin, N., Zoizner, G., Herman, A., Ougortsin, V., and Gefen, A., 2010. Use of weight-
 369 bearing MRI for evaluating wheelchair cushions based on internal soft-tissue deformations
 370 under ischial tuberosities, *Journal of Rehabilitation Research & Development*, 47(1):31–42.

371 Sopher, R, Nixon, J., Gorecki, C., and Gefen, A., 2010. Exposure to internal muscle tissue
 372 loads under the ischial tuberosities during sitting is elevated at abnormally high or low body
 373 mass indices. *Journal of Biomechanics*, 43:280–286.

374 Verver, M.M., van Hoof, J., Oomens, C.W.J., Wismans, J.S.H.M. and Baaijens, F.P.T., 2004.
375 A Finite Element Model of the Human Buttocks for Prediction of Seat Pressure Distributions,
376 Computer Methods in Biomechanics and Biomedical Engineering, 7(4):193-203.

377 Yushkevich, P.A., Piven, J., Hazlett, H.C., Gimpel Smith, R., Ho, S., Gee, J.C., and Gerig, G.,
378 2006. User-guided 3D active contour segmentation of anatomical structures: Significantly
379 improved efficiency and reliability. Neuroimage, 31(3):1116-28.

380

381

Figure captions:

Figure 1. (a) Finite element model of the buttocks, (b) and (c) Frontal and sagittal cross sections showing the three layers of materials defining the buttocks model: skin (in grey), fat (in yellow) and muscles (in red), the bones are represented in white and are simulated as fixed nodes, (d) CT scan slice showing the ischial tuberosity surrounded by muscles and fat tissues.

Figure 2. Pressure map measured with the Zebris platform. In this example, the maximum pressure (in red) is 4 N.cm^{-2} due to a non-symmetrical posture of the subject.

Figure 3. Pressure map corresponding to the subject's weight being only applied on his right side. The maximal pressure reaches 5 N.cm^{-2} (in red).

Figure 4. Evolution of the maximal internal strain as a function of the Young moduli chosen for the skin, fat, and muscle tissues.

Figure 5. The 57.4 % maximal Von Mises strains (red dots) are mainly located in the fat layer under the ischial tuberosities at the interface with the muscle layer: (a) view from the back, (b), view from the side.

398

399

400

401

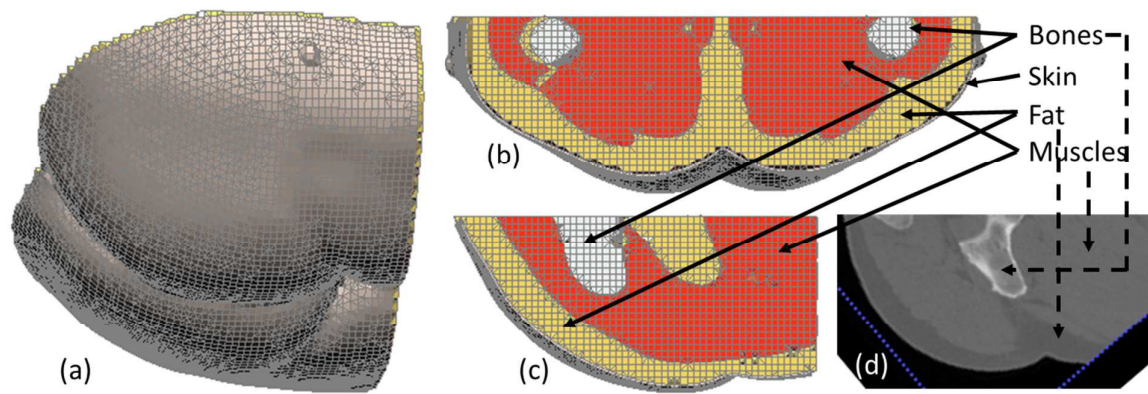
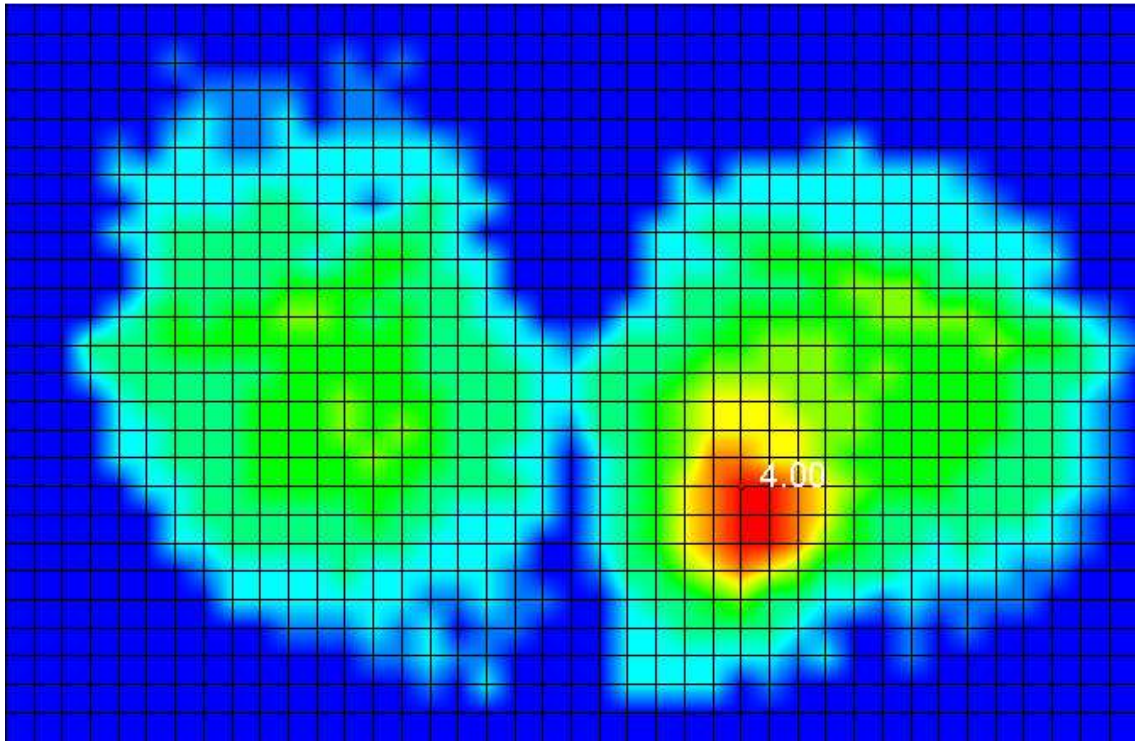


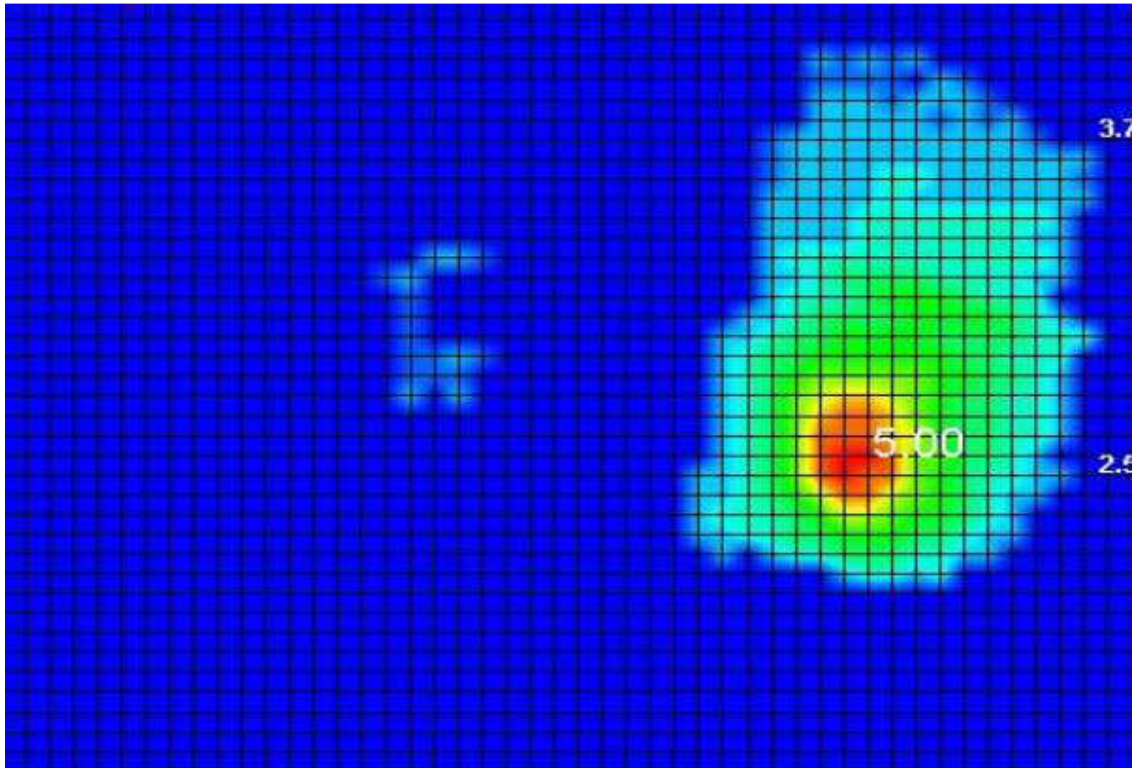
Figure 1



402

403 **Figure 2**

404

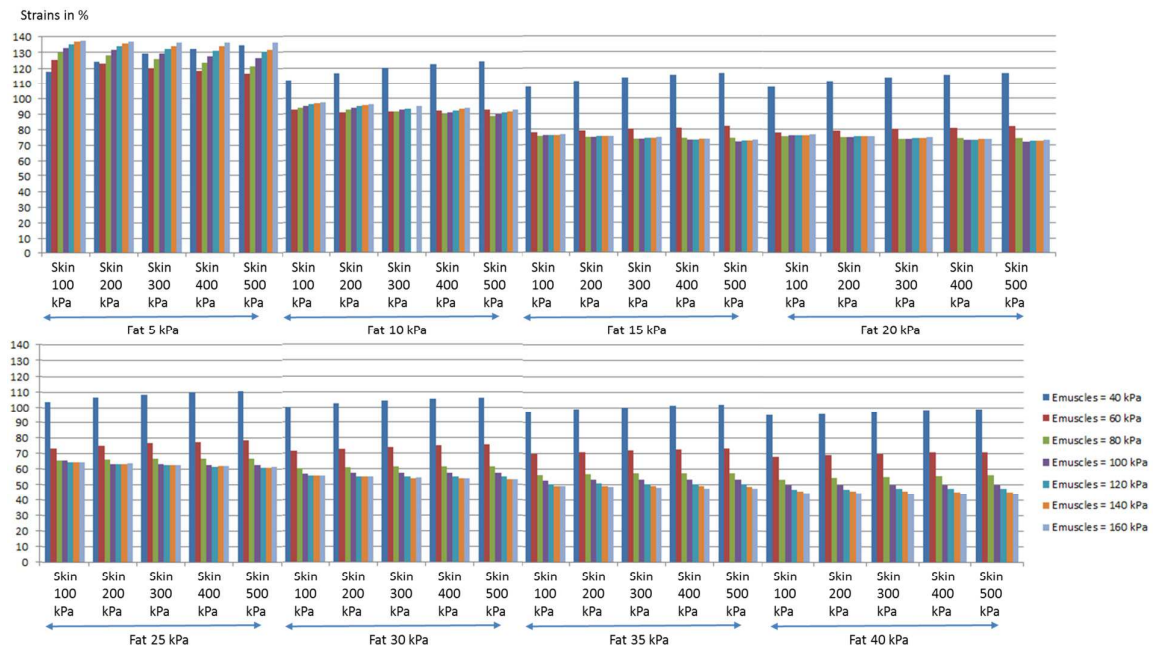


405

406 **Figure 3**

407

408



409

410 **Figure 4**

411

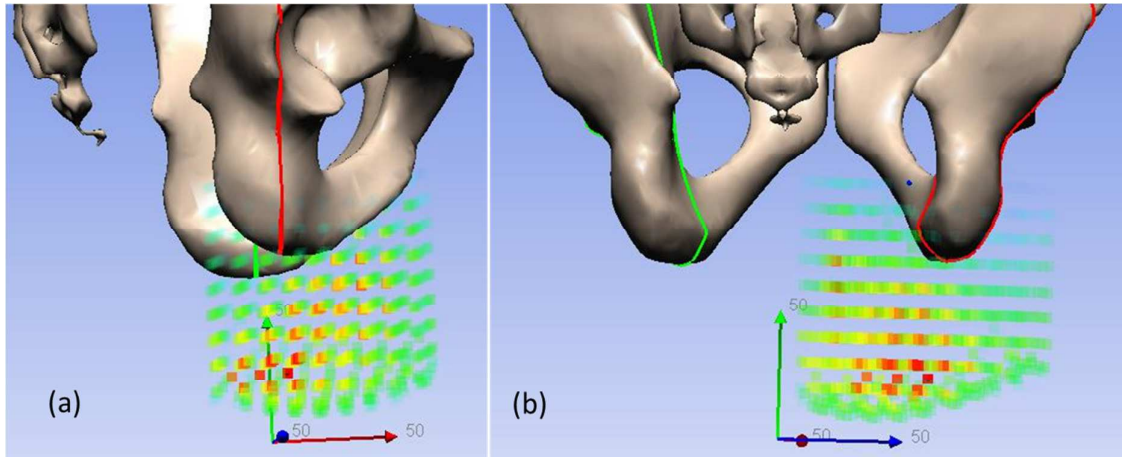


Figure 5